THE JOURNAL OF BIOLOGICAL CHEMISTRY VOL. 287, NO. 51, pp. 42784–42794, December 14, 2012

Rab26 Modulates the Cell Surface Transport of α_2-Adrenergic Receptors from the Golgi*

Received for publication, August 15, 2012, and in revised form, October 9, 2012 Published, JBC Papers in Press, October 26, 2012, DOI 10.1074/jbc.M112.410936

Chunman Li, Yi Fan, Tien-Hung Lan, Nevin A. Lambert, and Guangyu Wu[1]

From the Department of Pharmacology and Toxicology, Georgia Health Sciences University, Augusta, Georgia 30912

Background: Mechanisms underlying the cell surface export of G protein-coupled receptors (GPCRs) are poorly understood.
Results: Rab26 modulates the Golgi to cell surface transport of α_2-adrenergic receptors (α_2-ARs) and interacts with the receptors.
Conclusion: Rab26 controls the post-Golgi traffic of α_2-ARs via a physical interaction.
Significance: Rab26 functions as an important regulator for anterograde transport of GPCRs.

The molecular mechanisms underlying the transport from the Golgi to the cell surface of G protein-coupled receptors remain poorly elucidated. Here we determined the role of Rab26, a Ras-like small GTPase involved in vesicle-mediated secretion, in the cell surface export of α_2-adrenergic receptors. We found that transient expression of Rab26 mutants and siRNA-mediated depletion of Rab26 significantly attenuated the cell surface numbers of α_{2A}-AR and α_{2B}-AR, as well as ERK1/2 activation by α_{2B}-AR. Furthermore, the receptors were extensively arrested in the Golgi by Rab26 mutants and siRNA. Moreover, Rab26 directly and activation-dependently interacted with α_{2B}-AR, specifically the third intracellular loop. These data demonstrate that the small GTPase Rab26 regulates the Golgi to cell surface traffic of α_2-adrenergic receptors, likely through a physical interaction. These data also provide the first evidence implicating an important function of Rab26 in coordinating plasma membrane protein transport.

G protein-coupled receptors (GPCRs)[2] constitute the largest superfamily of the cell surface receptors and modulate a variety of cell functions largely via coupling to heterotrimeric G proteins, which in turn activate downstream effectors (1–3). One important factor that determines the magnitude of signaling initiated by a given receptor in cell is the amount of the receptor expressed at the cell surface available for binding to its cognate ligands. The level of receptor expression at the cell surface at the steady state is controlled by a number of elaborately regulated trafficking processes such as anterograde export of newly synthesized receptors to the cell surface, the endocytosis of the cell surface receptors to endosomes upon agonist stimulation, the recycling of the internalized receptor from endosomes to the cell surface, and the transport of receptors to lysosome for degradation (4). However, compared with the extensive studies on the events involved in the endocytosis, recycling, and degradation pathways (5–11), the molecular mechanisms governing the cell surface transport of GPCRs, especially from the Golgi, are poorly understood.

It has become apparent that GPCR transport from the Golgi to the cell surface is a regulated process. Similar to export from the ER, GPCR exit from the Golgi is controlled by the structural features embedded within the receptors. We have previously demonstrated that the N-terminal YS motif specifically regulates the exit of α_2-adrenergic receptors (α_2-ARs) from the Golgi (12). There are three α_2-AR subtypes, designated as α_{2A}-AR, α_{2B}-AR, and α_{2C}-AR. Both α_{2A}-AR and α_{2B}-AR nicely express at the cell surface, whereas α_{2C}-AR cell surface expression depends on the cell types (13). Because the YS motif is highly conserved among the three α_2-AR subtypes in different species, it may provide a common signal directing the exit from the Golgi of this subgroup of adrenergic receptors. In addition, G protein-coupled olfactory and chemokine receptors are released from the ER but accumulated in the Golgi (14, 15), and the opsin mutant E150K is accumulated in the *cis* and *medial* Golgi (16). Recent studies have also revealed that Ras-like small GTPases may play important roles in the Golgi to cell surface transport of GPCRs (17–22).

Rab GTPases are the largest branch of the Ras-related GTPase superfamily, consisting of more then 60 members in mammals, and regulate almost every step of vesicle-mediated protein transport, particularly the targeting, tethering, and fusion of transport vesicles with the appropriate acceptor membrane. Some Rab GTPases are expressed in specialized cells and modulate specific types of membrane trafficking. For example, Rab26 was found on the parotid acinar cell secretory granules to regulate amylase release (23, 24). Rab26 was also shown to interact with Rim1, a Rab3-interacting protein (25). Interestingly, a recent study demonstrated that the expression of Rab26 was regulated by the transcriptional factor MIST1 and was associated with the maturation of secretory granules (26). In a continuing effort to search for small GTPases in controlling export trafficking of GPCRs, we determined the role of Rab26 by using α_2-ARs as representatives. We found that Rab26 is able to regulate the cell surface transport, specifically from the

* This work was supported, in whole or in part, by National Institutes of Health Grants R01GM076167 (to G. W.) and R01GM096762 and R01GM078319 (to N. A. L.).

[1] To whom correspondence should be addressed: Dept. of Pharmacology and Toxicology, Georgia Health Sciences University, Augusta, GA 30912. Tel.: 706-721-0999; Fax: 706-721-2347; E-mail: guwu@georgiahealth.edu.

[2] The abbreviations used are: GPCR, G protein-coupled receptor; AR, adrenergic receptor; BRET, bioluminescence resonance energy transfer; ER, endoplasmic reticulum; ICL, intracellular loop; CT, C terminus.

Golgi, of α_2-ARs, and this function is likely mediated by its direct and activation-dependent interaction with the receptors.

EXPERIMENTAL PROCEDURES

Materials—N-terminal 3× HA-tagged human α_{2A}-AR (HA-α_{2A}-AR) and HA-α_{2B}-AR were obtained from Missouri S & T cDNA Resource Center (Rolla, MO). Antibodies against GFP and α_{2B}-AR were purchased from Santa Cruz Biotechnology, Inc. (Santa Cruz, CA). HA antibody 12CA5, G418, complete Mini protease inhibitor mixture, and FuGENE HD transfection reagent were from Roche Applied Science (Indianapolis, IN). Antibodies against ERK1/2 and phospho-ERK1/2 were from Cell Signaling Technology, Inc. (Beverly, MA). Rab26 and giantin antibodies were from Abcam (Cambridge, MA). [^{3}H]RX821002 (specific activity = 50 Ci/mmol) was from PerkinElmer Life Sciences. Alexa Fluor 488-, 594-, and 647-labeled secondary antibodies, Lipofectamine 2000 transfection reagent, and prolong antifade reagent containing DAPI were from Invitrogen. UK14304 was obtained from Sigma-Aldrich. MagneGST glutathione particles were from Promega (Madison, WI). All other materials were obtained as described previously (18, 27, 28).

Plasmid Constructions—Human α_{2B}-AR tagged with GFP at its C terminus (CT) (α_{2B}-AR-GFP) in the pEGFP-N1 vector was generated as described previously (12). The ORF of Rab26 was obtained by RT-PCR using total RNA extracted from HEK293 cells and the forward primer 5′-GAATTCTCCAGGAAGAAGACCCCCAAG-3′ and the reverse primer 5′-GGATCCTCAAGGGCGGCAGCAGGAGG-3′. The ORF was then digested with the restriction enzymes EcoRI and BamHI and subcloned in frame into the pEGFP-C1 vector. Rab26 was also cloned into the pDsRed-monomer-C1 vector using the same restriction sites. To generate GST fusion proteins encoding the first (ICL1, 10 residues from Thr-39 to Leu-48) and second (ICL2, 15 residues from Trp-112 to Pro-126) intracellular loops and the CT (24 residues from Thr-427 to Trp-450) of α_{2B}-AR, oligonucleotides containing the BamHI and XhoI restriction sites and encoding the ICL1, the ICL2 or the CT were synthesized, annealed, and ligated into the pGEX-4T-1 vector. To generate GST fusion proteins encoding the third intracellular loop (ICL3, 169 residues from Arg-194 to Val-372) of α_{2B}-AR, full-length α_{2B}-AR was amplified by PCR using the forward primer 5′-GCGGATCCCGCATCTACCTGATCGCCAAACG-3′ and the reverse primer 5′-GCCTCGAGTCACACGAAGGTGAAGCGCTTCTCCC-3′. The PCR product was digested with BamHI and XhoI and ligated into the pGEX-4T-1 vector. To generate the Rab26-Rluc8 construct, Rab6 was amplified by PCR using the forward primer 5′-GAATTCATGTCCAGGAAGAAGACCCCCAAG-3′ and the reverse primer 5′-GGATCCCGAGGGCGGCAGCAGGAGGCCCC-3′. The PCR product was digested with EcoRI and BamHI and then subcloned into the Rluc8-N1 vector. To construct α_{2B}-AR-Venus, α_{2B}-AR in the pEGFP-N1 vector was released by digestion using BamHI and Not1, and the fragment was subcloned into the Venus-1 vector. For *in vitro* translation, Rab26 was cloned into the pcDNA-3.1(−) vector at the EcoRI and BamHI restriction sites by PCR using the forward primer 5′-GAATTCATGTCCAGGAAGAAGACCCCCAAG-3′ and the reverse primer 5′-GGATCCTCAAGGGCGGCAGCAGGAGG. Rab mutants were generated using QuikChange site-directed mutagenesis (Agilent Technologies, La Jolla, CA). The structure of each construct used in the present study was verified by restriction mapping and nucleotide sequence analysis.

Generation of Cell Lines Stably Expressing α_{2B}-AR—HEK293 cells were cultured on 6-well dishes and transfected with 2 μg of HA-α_{2B}-AR in the pcDNA3.1(+) vector for 24 h using FuGENE HD transfection reagent according to the manufacturer's protocol. The cells were split into four 100-mm dishes and cultured for additional 24 h. The cells were then incubated with G418 at a concentration of 600 μg/ml for 2 weeks. Stable transfectants were isolated and grown in DMEM containing 300 μg/ml of G418. The cells stably expressing HA-α_{2B}-AR were confirmed by immunoblotting using HA antibodies and intact cell ligand binding using [^{3}H]RX821002 to quantify α_{2B}-AR expression at the cell surface as described below. Eight stable cell lines expressing different amounts of α_{2B}-AR were generated, and the cell line with the binding ability of 1.14×10^{-18} mol of [^{3}H]RX821002/cell was used in the current study.

Cell Culture and Transient Transfection—HEK293 and MCF-7 cells were cultured in DMEM with 10% fetal bovine serum, 100 units/ml of penicillin, and 100 μg/ml of streptomycin. Transient transfection of the cells was carried out using Lipofectamine 2000 as described previously (27). For transfection of HEK293 cells stably expressing HA-α_{2B}-AR, the cells were cultured on 6-well dishes and transfected with 1.8 μg of empty vectors or Rab constructs. For co-transfection, HEK293 cells were cultured on 6-well dishes and transfected with 0.2 μg of α_{2A}-AR plasmids together with 1.8 μg of empty vectors or Rab constructs. The transfection efficiency was estimated to be greater than 75% based on the GFP fluorescence.

For transient transfection of MCF-7 cells, the cells were cultured in 12-well dishes to 70–80% confluence and transfected with 1.0 μg of the pEGFP-C1 vector or Rab26N177I in the pEGFP-C1 vector. After 24 h, the cells were transferred to 6-well dishes and cultured for another 24 h. The cells were then transfected for the second time with 1.8 μg of the pEGFP-C1 vector or Rab26T177I. The experiments were performed at 60 h after the first transfection.

siRNA-mediated Knockdown of Rab26—Two Stealth™ RNAi duplexes (siRNA) targeting to human Rab26 (accession number NM_014353; number 1, 5′-GCUUCCGGCUGCAUGAUUACHUUAA-3′; number 2, 5′-UGGUCAGGAGCGGUUCCGCAGUGUU-3′) and an negative control med GC duplex were purchased from Invitrogen. HEK293 cells were cultured in 12-well dishes at a density of 1.5×10^5 cells/well for 24 h before transfection. Two μl of Lipofectamine 2000 and 1 μl of 20 μM siRNA were added separately into 50 μl of Opti-MEM medium. After incubation for 5 min, both solutions were mixed and incubated for 20 min. The transfection mixture was added to culture dishes containing 0.9 ml of fresh DMEM without antibiotics. After incubation at 37 °C for 6–8 h, the cells were split into 6-well dishes and cultured for additional 24 h. The cells were then transfected for the second time with 2.5 μl of 20 μM siRNA together with 400 ng of α_{2B}-AR. All of the experiments were performed at 72 h after the first siRNA transfection.

Confocal Fluorescence Microscopy—To visualize the subcellular distribution and co-localization of Rab26, giantin, and α_{2B}-AR, HEK293 cells grown on coverslips precoated with poly-L-lysine on 6-well dishes were transfected and fixed with 4% paraformaldehyde in PBS for 15 min. The cells were then permeabilized with 0.1% saponin for 20 min and blocked with PBS containing 5% BSA, 0.1% gelatin, and 0.1% saponin for 30 min. The cells were sequentially stained with primary antibodies and fluorophore-conjugated secondary antibodies. The coverslips were mounted with prolong antifade reagent (Invitrogen), and images were captured using a LSM510 Zessis confocal microscope equipped with a 63× objective (NA = 1.3).

For visualization of stably expressed HA-α_{2B}-AR, HEK293 cells were transfected and then fixed as described above. To permeabilize the cells, the cells were incubated with PBS containing 0.2% Triton X-100 for 5 min. The cells were then incubated with PBS containing 5% BSA and 0.1% gelatin for 30 min followed by staining with HA antibodies (1:1500 dilution) and Alexa 594-conjugated secondary antibodies (1:300 dilution).

Intact Cell Radioligand Binding—The cell surface expression of α_{2A}-AR and α_{2B}-AR was measured by ligand binding of intact live cells using the membrane-impermeable ligand [^{3}H]RX821002 as described previously (29, 30). Briefly, HEK293 cells cultured on 6-well dishes were transfected and then split into 12-well dishes. The cells were incubated with 300 μl of DMEM plus [^{3}H]RX821002 at a concentration of 20 nM for 90 min at room temperature. The cells were washed twice with 1 ml of ice-cold PBS, and the cell surface-bound ligands were extracted by 1 M NaOH treatment for 2 h. The nonspecific binding was determined in the presence of rauwolscine (10 μM). The radioactivity was counted by liquid scintillation spectrometry in 3.5 ml of Ecoscint A scintillation solution.

Measurement of ERK1/2 Activation—HEK293 cells were cultured on 6-well dishes and transfected with α_{2B}-AR together with individual Rab26 mutant or Rab26 siRNA as described above. The cells were starved for at least 3 h before stimulation with UK14304 at a concentration of 1 μM for 5 min. Stimulation was terminated by the addition of 200 μl of ice-cold cell lysis buffer containing 50 mM Tris-HCl, pH 7.4, 150 mM NaCl, 1% Nonidet P-40, 1 mM sodium orthovanadate, 1 mM β-glycerophosphate, and complete Mini protease inhibitor mixture. After solubilizing the cells on ice for 20 min, 15 μl of total cell lysates was separated by 12% SDS-PAGE. ERK1/2 activation was determined by measuring the levels of phosphorylation of ERK1/2 with phospho-specific ERK1/2 antibodies by immunoblotting (27).

Co-immunoprecipitation of α_{2B}-AR and Rab26—HEK293 cells stably expressing HA-α_{2B}-AR were cultured on 100-mm dishes and transfected with 8 μg of the pEGFP-C1 vector or Rab26 in the pEGFP-C1 vector for 48 h. The cells were washed twice with PBS, harvested, and lysed with 500 μl of lysis buffer containing 50 mM Tris-HCl, pH 7.4, 150 mM NaCl, 1% Nonidet P-40, and complete Mini protease inhibitor mixture. After gentle rotation for 1 h at 4 °C, samples were centrifuged for 15 min at 14,000 × *g*. The supernatants were diluted with equal volume of buffer containing 50 mM Tris-HCl, pH 7.4, 150 mM NaCl, and 0.5% gelatin and then incubated with 1 μg of α_{2B}-AR antibodies overnight at 4 °C with gentle rotation followed by incubation with 50 μl of protein G-Sepharose 4B beads for 5 h. Resin was collected by centrifugation and washed four times each with 1 ml of lysis buffer. Immunoprecipitated receptors were eluted with 30 μl of 1× SDS gel loading buffer, and 20 μl from each sample was separated by SDS-PAGE to probe for GFP-Rab26 in the immunoprecipitates by immunoblotting using GFP antibodies (1:3000 dilution). In parallel, each sample was further diluted five times with 1× SDS gel loading buffer, separated by SDS-PAGE, and probed with HA antibodies (1:3000 dilution) to determine the amount of HA-α_{2B}-AR in the immunoprecipitates.

Bioluminescence Resonance Energy Transfer (BRET) Assays—The live cell-based BRET assay to measure the possible interaction between α_{2B}-AR and Rab26 was carried out as described previously (31). HEK293 cells were cultured on 6-well dishes and transfected with 0.1 μg of Rab26-Rluc8 and 1.5 μg of α_{2B}-AR-Venus for 24 h. The cells were then harvested and transferred to black 96-well plates. Coelenterazine h (5 mM) was added to all wells immediately prior to making measurements. Luminescence measurements were made using a Mithras LB940 photon-counting plate reader (Berthold Technologies GmbH, Bad Wildbad, Germany). Raw BRET signals were calculated by dividing the emission intensity at 520–545 nm by the emission intensity at 475–495 nm. Net BRET was this ratio minus the same ratio measured from cells expressing only the BRET donor (Rluc8).

GST Fusion Protein Pulldown Assays—The interaction of the intracellular domains of α_{2B}-AR with Rab26 was measured by using the MagneGST pulldown system as described essentially (18, 28). Briefly, GST fusion proteins were expressed in BL21 bacteria and purified using MagneGST glutathione particles. Immobilized fusion proteins were either used immediately or stored at 4 °C for no longer than 3 days. Each batch of fusion proteins used in experiments was first analyzed by Coomassie Brilliant Blue staining following SDS-PAGE. HEK239 cells were transiently transfected with GFP-tagged Rab26 or its individual mutant, and the total HEK293 cell homogenates were incubated with GST fusion proteins tethered to the glutathione particles in 500 μl of binding buffer containing 20 mM Tris-HCl, pH 7.5, 140 mM NaCl, 1% Nonidet P-40, and 0.5% BSA for 4 h at 4 °C. The particles were washed four times with 0.5 ml of binding buffer, and the retained proteins were solubilized in 1× SDS gel loading buffer. GFP-Rab26 bound to the GST fusion proteins was detected by immunoblotting using GFP antibodies.

Translation of Rab26 in Vitro—Rab26 in the pcDNA3.1(−) vector was translated using the TnT T7 quick *in vitro* translation system (Promega) according to the manufacturer's protocol. Briefly, the reaction was carried out in a total volume of 50 μl containing 40 μl of TnT T7 Quick Master Mix, 1 μl of 1 mM methionine, and 1 μg of the Rab26 plasmid at 30 °C for 90 min. After translation, 20 μl of the reaction mixtures was diluted into 200 μl of binding buffer containing 20 mM Tris-HCl, pH 7.5, 140 mM NaCl, 1% Nonidet P-40, and 0.5% BSA. Rab26 was then incubated in binding buffer containing 100 μM GTPγS or GDP for 1 h at room temperature followed by incubation with GST fusion proteins tethered to MagneGST particles as described above.

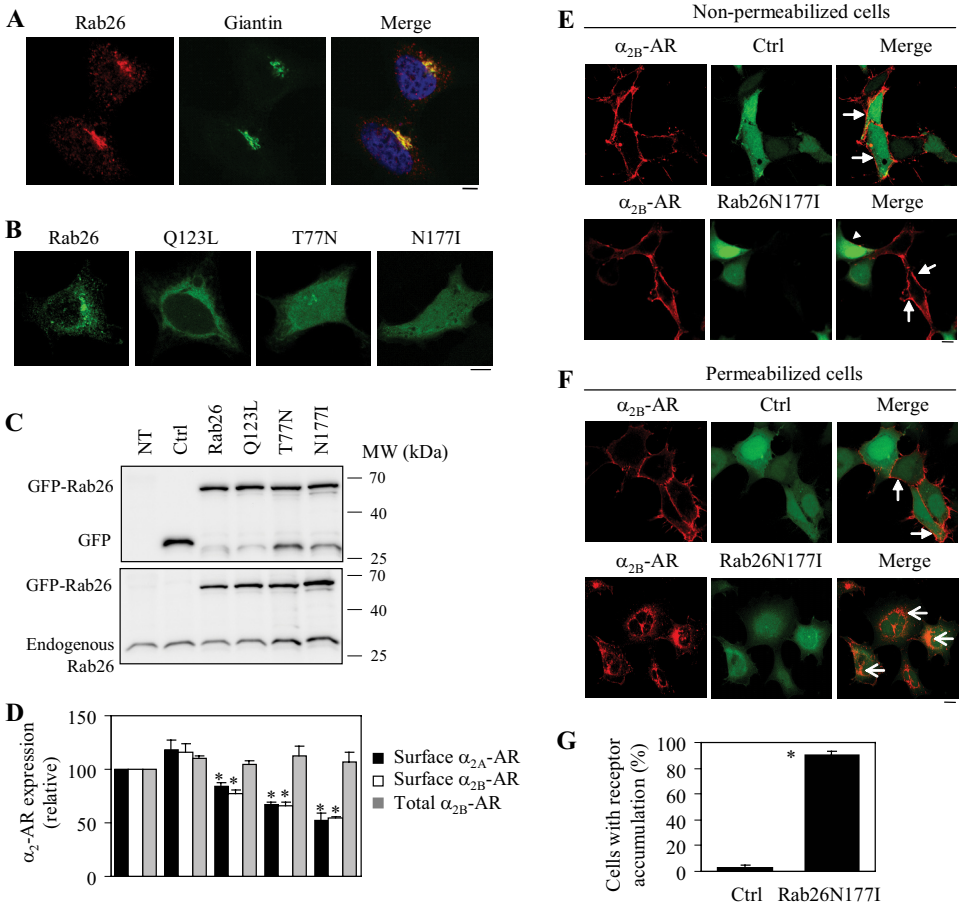

FIGURE 1. **Effect of transient expression of Rab26 and its mutants on the cell surface expression of both α_{2A}-AR and α_{2B}-AR.** *A*, co-localization of endogenous Rab26 with the Golgi marker giantin. HEK293 cells cultured on coverslips were stained with Rab26 (1:100 dilution) and giantin (1:500 dilution) antibodies followed by staining with Alexa 594- and 488-conjugated secondary antibodies (1:300 dilution). Co-localization of Rab26 and giantin was revealed by confocal microscopy. *Red*, Rab26; *green*, giantin; *yellow*, co-localization of Rab26 and giantin. *B*, subcellular distribution of Rab26 and its mutants Q123L, T77N, and N177I. GFP-tagged Rab26 and its mutants were expressed in HEK293 cells, and their subcellular distribution was detected by confocal microscopy. *C*, Western blot analysis of the expression of Rab26 and its mutants. HEK293 cells were cultured on 6-well plates and transfected with the pEGFP-C1 vector (*Ctrl*), Rab26, or individual Rab26 mutant tagged with GFP. Total cell homogenates were separated by 12% SDS-PAGE, and the expression of Rab26 was detected by immunoblotting using GFP (*upper panel*) and Rab26 antibodies (*lower panel*). *NT*, nontransfection. The molecular mass (*MW*) markers (kDa) are indicated on the *right*. The apparent molecular masses of GFP-Rab26, GFP and endogenous Rab26 are ~56, 27, and 27 kDa, respectively. *D*, effect of Rab26 and its mutants on the cell surface expression of α_{2A}-AR and α_{2B}-AR. HEK293 cells stably expressing α_{2B}-AR were transfected with GFP-Rab26, and α_{2A}-AR and GFP-Rab26 were transiently co-expressed in HEK293 cells. The cell surface expression of α_{2A}-AR and α_{2B}-AR was determined by intact cell ligand binding using [^{3}H]RX821002 at a concentration of 20 μM as described under "Experimental Procedures." The nonspecific binding was determined in the presence of rauwolscine (10 μM). The mean values of specific [^{3}H]RX821002 binding were 13,240 ± 530 and 25,589 ± 3716 cpm from control cells expressing α_{2A}-AR and α_{2B}-AR, respectively. The total α_{2B}-AR expression was measured by flow cytometry measuring the GFP signal in cells transfected with GFP-tagged α_{2B}-AR together with individual Rab26. The data shown are percentages of the mean values obtained from control cells and are presented as the means ± S.E. of at least three different experiments each in triplicate. *, $p < 0.05$ *versus Ctrl*. *E* and *F*, effect of Rab26N177I on the subcellular distribution of α_{2B}-AR in nonpermeabilized (*E*) and permeabilized cells (*F*). HEK293 cells stably expressing HA-α_{2B}-AR were cultured on coverslips and transfected with the pEGFP-C1 vector (*Ctrl*) or GFP-tagged Rab26N177I. In *F*, the cells were treated with 0.2% Triton X-100 for 5 min. The subcellular distribution of α_{2B}-AR was revealed by confocal microscopy following sequential staining with HA antibodies (1:1500 dilution) and Alexa 594-conjugated secondary antibodies as described under "Experimental Procedures." *Red*, HA-α_{2B}-AR; *green*, GFP (*upper panels*) or GFP-Rab26N177I (*lower panels*). *Closed arrows* indicate the cell surface expression of α_{2B}-AR; an *arrowhead* indicates the reduction of the cell surface α_{2B}-AR in a cell expressing GFP-Rab26N177I; *open arrows* show extensive accumulation of α_{2B}-AR in permeabilized cells expressing GFP-Rab26N177I. In *A*, *B*, *E*, and *F*, the data shown are representative images of at least three independent experiments. *Scale bars*, 10 μm. *G*, quantitative data of *F*. The data shown are percentages of the mean values and are presented as the means ± S.E. of three different experiments.

Statistical Analysis—Differences were evaluated using Student's *t* test, and $p < 0.05$ was considered as statistically significant. The data are expressed as the means ± S.E.

RESULTS

Effects of Rab26 and Its Mutants on the Cell Surface Transport of α_{2A}-AR and α_{2B}-AR—We first studied the subcellular distribution of endogenous Rab26 and exogenously expressed GFP-tagged Rab26 and its constitutively active and dominant-negative mutants in HEK293 cells. As revealed by confocal microscopy, endogenous Rab26 was strongly co-localized with giantin, a Golgi marker, in HEK293 cells (Fig. 1*A*). The subcellular distribution of GFP-tagged Rab26 was very much similar to endogenous Rab26 (Fig. 1*B*). Consistent with the subcellular distribution of many other Rab mutants, the GTP-bound mutant Rab26Q123L was largely localized to the perinuclear region, whereas the GDP-bound mutant Rab26T77N and the guanine nucleotide binding-deficient Rab26N177I were predominantly expressed in the cytoplasm (Fig. 1*B*).

We then determined the effect of transient expression of Rab26 and all three Rab26 mutants on the cell surface expression of both α_{2A}-AR and α_{2B}-AR. The expression of Rab26 and its mutants was measured by immunoblotting using both GFP and Rab26 antibodies (Fig. 1*C*), and the cell surface expression of α_{2A}-AR and α_{2B}-AR was determined by ligand binding in intact live cells using the radioligand [^{3}H]RX821002. Transient expression of all three Rab26 mutants significantly inhibited the cell surface expression of α_2-ARs with the order of N177I > T77N > Q123I, and the inhibitory effects were very similar between α_{2A}-AR and α_{2B}-AR (Fig. 1*D*). In contrast, expression of wild-type Rab26 only moderately enhanced the cell surface expression of both receptors and expression of Rab26 mutants did not significantly alter the total expression of α_{2B}-AR (Fig. 1*D*).

To confirm the inhibitory effect of the Rab26 mutants on the cell surface expression of α_2-ARs as measured by intact cell ligand binding, the subcellular distribution of HA-α_{2B}-AR was then visualized by confocal microscopy after staining with anti-HA antibodies. In nonpermeabilized cells, α_{2B}-AR was robustly expressed at the cell surface in cells expressing GFP alone, whereas the cell surface expression of α_{2B}-AR was markedly attenuated in cells expressing Rab26N177I (Fig. 1*E*). In Triton X-100-treated cells, expression of Rab26N177I induced an extensive accumulation of α_{2B}-AR in a discrete compartment in the perinuclear region (Fig. 1*F*). Quantitative analysis showed that ~3 and 90% cells had intracellular accumulation of the receptor in cells expressing GFP and GFP-tagged Rab26N177I, respectively (Fig. 1*G*). These data demonstrate that Rab26 is required for the cell surface transport of α_2-ARs.

Inhibition of the Cell Surface Expression of α_{2A}-AR and α_{2B}-AR by siRNA-mediated Knockdown of Rab26—We next determined the effect of siRNA-mediated depletion of endogenous Rab26 on the cell surface targeting of both α_{2A}-AR and α_{2B}-AR. Introduction of each Rab26 siRNA markedly and specifically knocked down Rab26 by ~90% without affecting the expression of the closely related small GTPase Rab4 and β-actin when compared with cells transfected with control siRNA and cells without transfection (Fig. 2, *A* and *B*). siRNA-mediated knockdown of Rab26 strongly inhibited the cell surface expression of both α_{2A}-AR and α_{2B}-AR as measured by intact cell ligand binding (Fig. 2*C*). In contrast, siRNA-mediated knockdown of Rab26 did not significantly influence the overall expression of α_{2B}-AR (Fig. 2*C*). Subcellular distribution analysis showed that expression of Rab26 siRNA arrested α_{2B}-AR in the intracellular compartments, and the receptors were unable to transport to the cell surface (Fig. 2*D*). These data further suggest that the normal function of Rab26 is essential for the cell surface movement of α_{2A}-AR and α_{2B}-AR.

Effect of Rab26 Mutants and Rab26 siRNA on the Cell Surface Expression of Endogenous α_2-ARs—Similar to the results obtained in HEK293 cells transfected with exogenous α_{2A}-AR and α_{2B}-AR, transient expression of the dominant-negative mutant Rab26N177I (Fig. 3*A*) significantly inhibited the cell surface expression of endogenous α_2-ARs in MCF-7 cells by 45% as measured by intact cell ligand binding (Fig. 3*B*). Expression of each Rab26 siRNA to knockdown Rab26 (Fig. 3, *C* and *D*) also significantly reduced the cell surface expression of endogenous α_2-ARs by ~35% (Fig. 3*E*). These data demonstrate an important role of Rab26 in the cell surface transport of endogenous α_2-ARs.

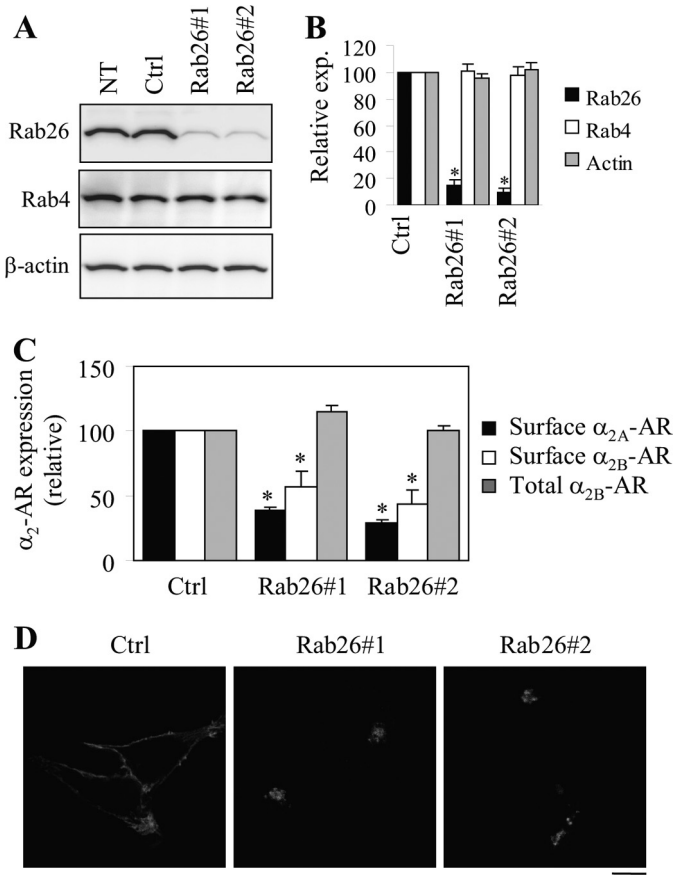

FIGURE 2. **Effect of siRNA-mediated knockdown of Rab26 on the cell surface expression of α_{2A}-AR and α_{2B}-AR.** *A*, siRNA-mediated knockdown of Rab26. HEK293 cells cultured on 6-well dishes were transiently transfected with control siRNA (*Ctrl*) or individual Rab26 siRNA. Expression of Rab26, Rab4, and β-actin was measured by immunoblotting. The apparent molecular masses of endogenous Rab26, Rab4, and β-actin are ~27, 24, and 42 kDa, respectively. *B*, quantitative data shown in *A*. *C*, effect of siRNA-mediated knockdown of Rab26 on the cell surface expression of α_{2A}-AR and α_{2B}-AR. HEK293 cells stably expressing α_{2B}-AR were transfected with control (*Ctrl*) or Rab26 siRNA, and α_{2A}-AR and siRNA were transiently co-expressed in HEK293 cells. The cell surface expression of α_2-ARs was determined by intact cell ligand binding using [^{3}H]RX821002 as described under "Experimental Procedures." The total α_{2B}-AR expression was measured by flow cytometry measuring the GFP signal in cells transfected with GFP-tagged α_{2B}-AR together with individual siRNA. In *B* and *C*, the data shown are percentages of the mean values obtained from cells transfected with control siRNA and are presented as the means ± S.E. of three different experiments. *, $p < 0.05$ *versus* respective control. *D*, effect of Rab26 siRNA on the subcellular distribution of α_{2B}-AR. HEK293 cells cultured on coverslips were transfected with GFP-tagged α_{2B}-AR together with control or Rab26 siRNA, and the subcellular distribution of α_{2B}-AR was revealed by confocal microscopy. The data shown are representative images of at least four independent experiments. *Scale bar*, 10 μm. *NT*, nontransfection.

Effect of Rab26 Mutants and Rab26 siRNA on ERK1/2 Activation by α_{2B}-AR—To define whether the attenuated α_2-AR expression at the cell surface caused by expression of Rab26 mutants or Rab26 siRNA could result in a concomitant defective signaling, we measured the activation of the mitogen-activated protein kinase pathway, specifically ERK1/2, in response to stimulation with the α_2-AR agonist UK14304. ERK1/2 activation by UK14304 was significantly compromised in cells

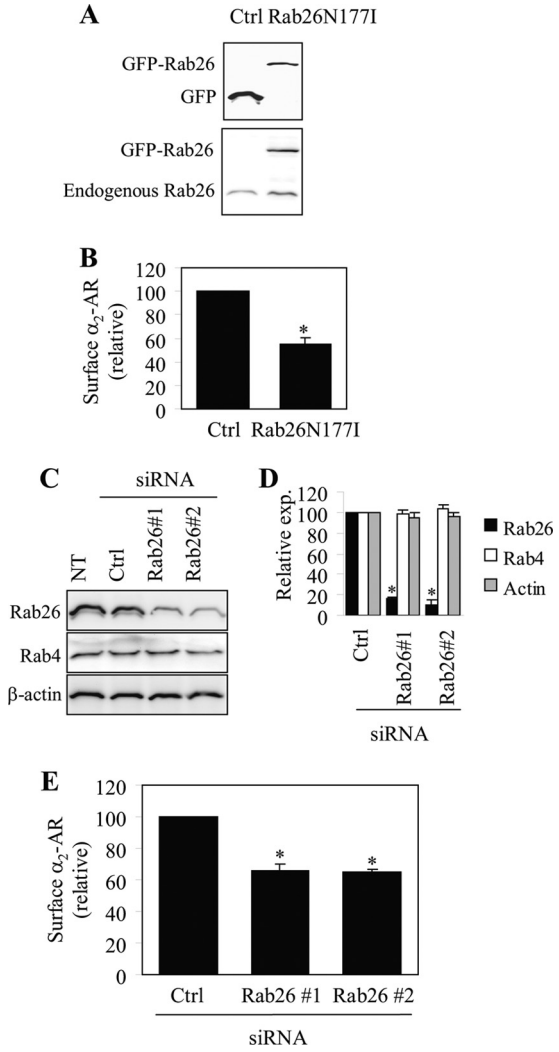

FIGURE 3. **Effect of transient expression of Rab26N177I and siRNA-mediated knockdown of Rab26 on the cell surface expression of endogenous α_2-ARs in MCF-7 cells.** *A*, Western blot analysis of Rab26N177I expression. MCF-7 cells were transfected with the pEGFP-C1 vector (*Ctrl*) or GFP-tagged Rab26N177I and Rab26 expression was measured by immunoblotting using GFP (*upper panel*) and Rab26 antibodies (*lower panel*). Similar results were obtained in three experiments. *B*, effect of Rab26N177I on the cell surface expression of endogenous α_2-ARs as measured by intact cell ligand binding using [^{3}H]RX821002 as described under "Experimental Procedures." *C*, siRNA-mediated knockdown of Rab26. MCF-7 cells were transiently transfected with control siRNA (*Ctrl*) or individual Rab26 siRNA, and the expression of Rab26, Rab4, and β-actin was measured by immunoblotting. *D*, quantitative data shown in *C*. *E*, effect of siRNA-mediated knockdown of Rab26 on the cell surface expression of α_2-ARs as measured by intact cell ligand binding. The mean values of specific [^{3}H]RX821002 binding were 760 $\pm$ 69 and 561 $\pm$ 72 cpm from cells transfected with the pEGFP-C1 vector and control siRNA, respectively. In *B*, *D*, and *E*, the data shown are percentages of the mean values obtained from cells transfected with control vector or control siRNA and are presented as the mean $\pm$ S.E. of three individual experiments. *, $p < 0.05$ *versus* control.

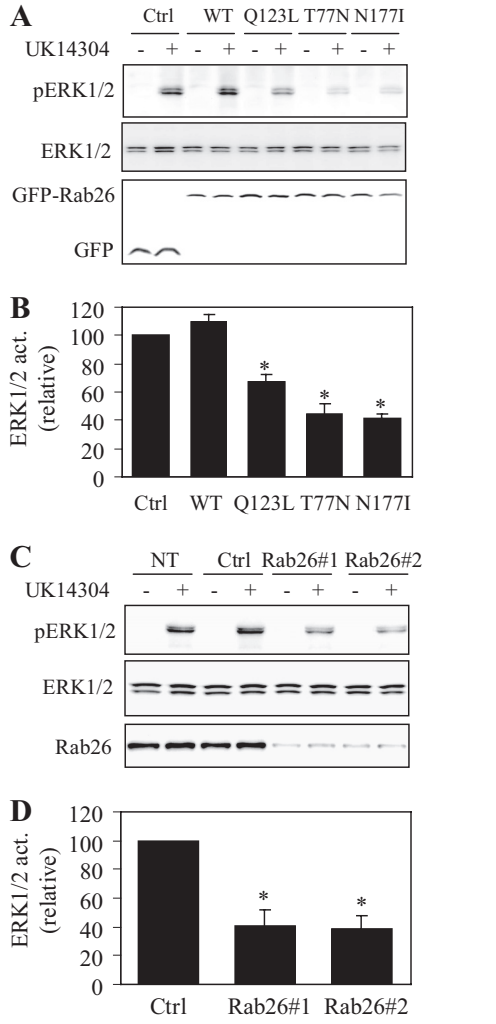

FIGURE 4. **Effect of transient expression of Rab26 mutants and siRNA-mediated knockdown of Rab26 on α_{2B}-AR-mediated ERK1/2 activation.** *A*, effect of Rab26 on α_{2B}-AR-mediated ERK1/2 activation. HEK293 cells stably expressing α_{2B}-AR were transfected with the pEGFP-C1 vector (*Ctrl*), GFP-tagged wild-type Rab26 (*WT*), or individual Rab26 mutant. The cells were stimulated with UK14304 at a concentration of 1 μM for 5 min, and ERK1/2 activation was determined by immunoblotting using phospho-specific ERK1/2 antibodies. *B*, quantitative data shown in *A*. *C*, effect of siRNA-mediated knockdown of Rab26 on α_{2B}-AR-mediated ERK1/2 activation. HEK293 cells stably expressing α_{2B}-AR were transfected with control siRNA (*Ctrl*) or Rab26 siRNA and stimulated with UK14304 as described above. *NT*, nontransfection. *D*, quantitative data shown in *C*. In *A* and *C*, *top panels*, representative blots showing ERK1/2 activation; *middle panels*, total ERK1/2 expression; *bottom panels*, Rab26 expression. In *B* and *D*, the data are expressed as percentages of ERK1/2 activation obtained from control cells and are presented as the means $\pm$ S.E. of three experiments. *, $p < 0.05$ *versus* control.

expressing α_{2B}-AR together with individual Rab26 mutant, whereas expression of wild-type Rab26 only slightly enhanced ERK1/2 activation as compared with cells expressing α_{2B}-AR alone (Fig. 4, *A* and *B*). Furthermore, ERK1/2 activation by UK14304 was markedly blocked by each Rab26 siRNA as compared with cells transfected with control siRNA (Fig. 4, *C* and *D*). These data are consistent with the inhibitory effect of Rab26 mutants and Rab26 siRNA on the cell surface expression of α_{2B}-AR and suggest that Rab26 is able to modulate not only the trafficking but also the signaling of α_2-ARs.

Inhibition of Exit from the Golgi of α_{2B}-AR by Rab26 Mutants and Rab26 siRNA—To define the intracellular compartment in which Rab26 regulates α_2-AR transport, Rab26 and its mutants were tagged with DsRed. The subcellular distribution of DsRed-tagged Rab26 was almost identical to their GFP-tagged forms (Fig. 5*A*), suggesting that epitope tagging (*i.e.*, GFP and DsRed) did not have significant impacts on the subcellular localization of Rab26.

DsRed-tagged Rab26 or its mutant was expressed together with GFP-tagged α_{2B}-AR, and the co-localization of α_{2B}-AR

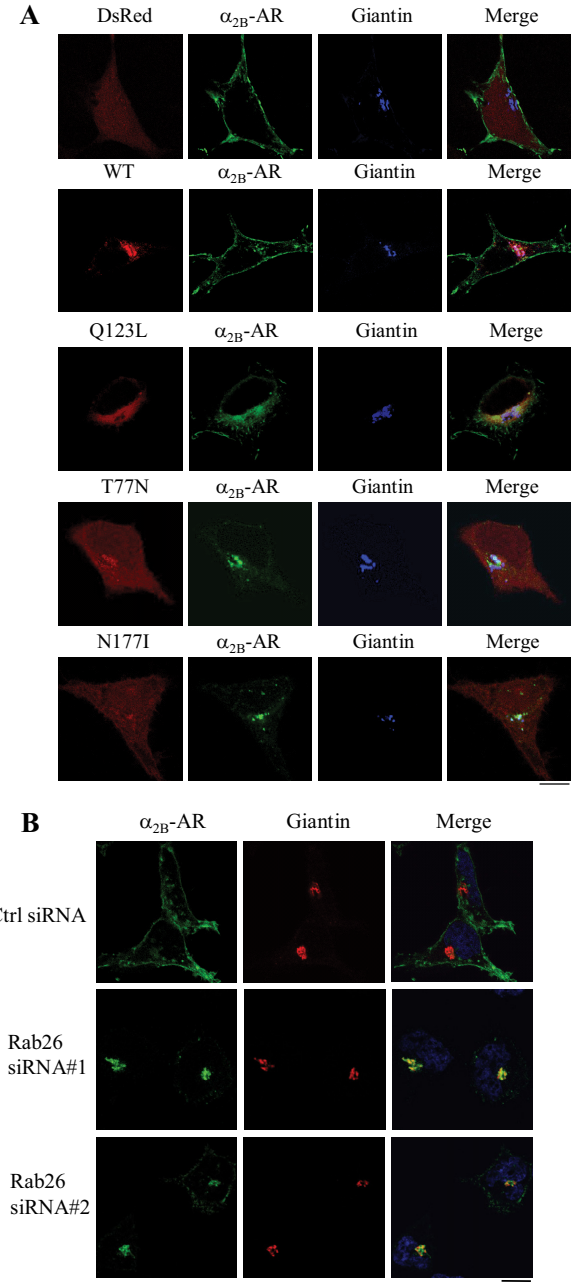

FIGURE 5. **Co-localization of α_{2B}-AR with the Golgi marker giantin.** *A*, co-localization of α_{2B}-AR with giantin in cells expressing Rab26 or its mutants. HEK293 cells cultured on coverslips were transfected with α_{2B}-AR-GFP together with the pDsRed-monomer-C1 vector, DsRed-tagged wild-type Rab26 (*WT*), or individual Rab26 mutant. Co-localization of α_{2B}-AR with the Golgi marker giantin was revealed by confocal fluorescence microscopy following staining with giantin antibodies and Alexa Fluor 647-labeled secondary antibodies (1:300 dilution). *Red*, DsRed or DsRed-tagged Rab26; *green*, GFP-tagged α_{2B}-AR; *blue*, giantin. *B*, co-localization of α_{2B}-AR with giantin in cells expressing Rab26 siRNA. HEK293 cells were transfected with α_{2B}-AR-GFP together with control siRNA or Rab26 siRNA. The cells were then stained with giantin antibodies and Alexa Fluor 594-labeled secondary antibodies. *Green*, GFP-tagged α_{2B}-AR; *red*, giantin; *yellow*, co-localization of α_{2B}-AR with giantin. In *A* and *B*, the data shown are representative images of at least three independent experiments. *Scale bars*, 10 μm.

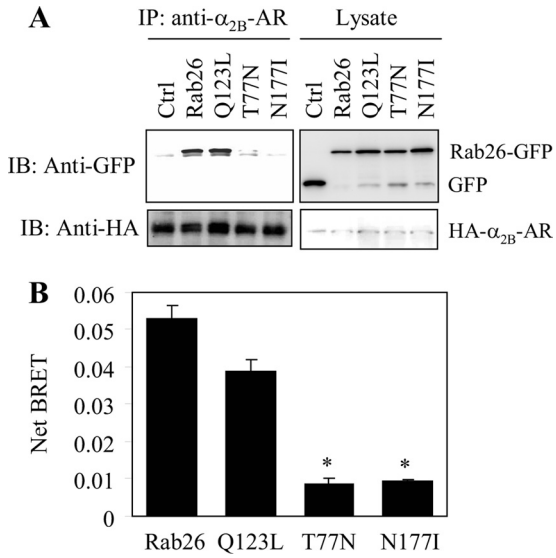

FIGURE 6. **Interaction of full-length α_{2B}-AR with Rab26.** *A*, interaction of α_{2B}-AR with Rab26 and its mutants as measured by co-immunoprecipitation. HEK293 cells stably expressing HA-α_{2B}-AR were transfected with the pEGFP-C1 vector (*Ctrl*) or GFP-tagged Rab26, and the receptors were immunoprecipitated (*IP*) with α_{2B}-AR antibodies as described under "Experimental Procedures." The level of Rab26 in the immunoprecipitates was determined by immunoblotting (*IB*) using GFP antibodies (*upper panel*), and the immunoprecipitated receptors were detected using HA antibodies (*lower panel*). The apparent molecular mass of HA-α_{2B}-AR is ~50 kDa. *B*, net BRET between α_{2B}-AR and Rab26. HEK293 cells were transiently transfected with Venus-tagged α_{2B}-AR together with Rluc-tagged Rab26 or individual Rab26 mutant, and the BRET between α_{2B}-AR and Rab26 was measured as described under "Experimental Procedures." The data are presented as the means ± S.E. of three individual experiments each in triplicate. *, $p < 0.05$ *versus* Rab26 or the GTP-bound mutant Q123L.

with different intracellular markers was visualized by confocal microscopy. α_{2B}-AR was clearly expressed at the cell surface in cells transfected with the pEGFP-C1 vector and wild-type Rab26. α_{2B}-AR was partially co-localized with the Golgi marker giantin in cells expressing Rab26Q123L. In contrast, α_{2B}-AR was remarkably co-localized with giantin, but not ER markers (data not shown), in cells transfected with Rab26T77N and Rab26N177I (Fig. 5*A*). Furthermore, α_{2B}-AR was also extensively co-localized with giantin but not ER markers (data not shown) in cells transfected with Rab26 siRNA (Fig. 5*B*). These data demonstrate that inhibition of Rab26 function by expressing Rab26 mutants and Rab26 siRNA induces defective α_{2B}-AR transport at the level of the Golgi.

Activation-dependent Interaction of Rab26 with Full Length α_{2B}-AR—To elucidate the possible molecular mechanisms underlying the function of Rab26 in regulating α_2-AR transport, we sought to define whether Rab26 is able to interact with α_{2B}-AR. In the first series of experiments, we determined the interaction of α_{2B}-AR with Rab26 and its three mutants by co-immunoprecipitation. HEK293 cells stably expressing HA-α_{2B}-AR were transiently transfected with GFP-Rab26, and HA-α_{2B}-AR was immunoprecipitated by α_{2B}-AR antibodies. The amounts of Rab26 in the immunoprecipitates detected by immunoblotting using GFP antibodies were much higher from cells expressing wild-type Rab26 and the active mutant Q123L than from cells expressing the dominant-negative mutants T77N and N177I (Fig. 6*A*).

In the second series of experiments, we used the BRET assay to measure whether Rab26 and α_{2B}-AR are in close proximity in live cells. HEK293 cells were transfected with Venus-tagged α_{2B}-AR and Rluc8-tagged Rab26 or individual Rab26 mutant. The net BRET between α_{2B}-AR and wild-type Rab26 or the

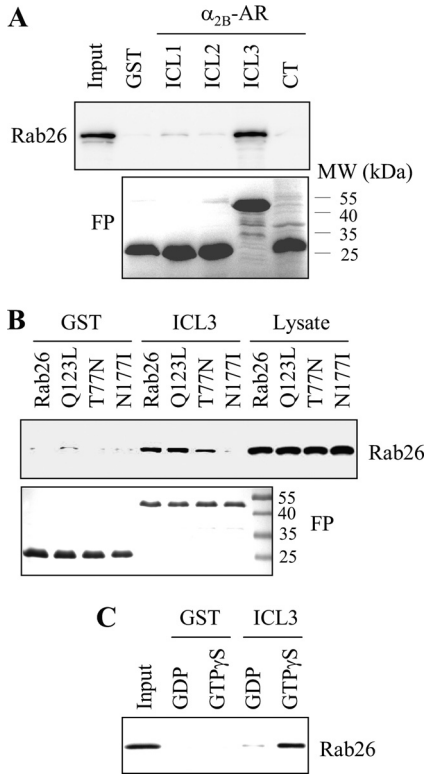

FIGURE 7. **Interaction of the third intracellular loop of α_{2B}-AR with Rab26.** *A*, interaction of the intracellular domains of α_{2B}-AR with Rab26 as measured by GST fusion protein pulldown assays. ICL1, ICL2, ICL3, and CT of α_{2B}-AR were generated as GST fusion proteins (*FP*) (*lower panel*). GFP-tagged Rab26 was expressed in HEK293 cells, and total cell homogenates were incubated with the purified GST fusion proteins as described under "Experimental Procedures." Rab26 bound to the GST fusion proteins was revealed by immunoblotting using GFP antibodies (*upper panel*). *B*, interaction of the α_{2B}-AR ICL3 with Rab26 and its mutants. GFP-tagged Rab26 and its mutants were transiently expressed in HEK293 cells, and their interaction with the GST-ICL3 fusion proteins (FP) (*lower panel*) was determined by the GST pulldown assay. Bound Rab26 was detected by immunoblotting using GFP antibodies (*upper panel*). *C*, direct and activation-dependent interaction of Rab26 with the α_{2B}-AR ICL3. Rab26 prepared by the *in vitro* translation system was incubated with 100 μM GTPγS or GDP for 1 h and then incubated with GST or the GST-ICL3 fusion proteins as described under "Experimental Procedures." In each panel, similar results were obtained in at least three different experiments. *MW*, molecular mass.

constitutively active mutant Rab26Q123L was significantly higher than those between α_{2B}-AR and the dominant-negative mutants Rab26T77N and Rab26N177I (Fig. 6*B*). These data reveal that α_{2B}-AR is able to form a complex with Rab26 GTPase, preferentially in its active GTP-bound form.

Direct and Activation-dependent Interaction of Rab26 with the Third Intracellular Loop of α_{2B}-AR—To identify the intracellular domain mediating α_{2B}-AR interaction with Rab26, the ICL1, the ICL2, the ICL3, and the CT of α_{2B}-AR were generated as GST fusion proteins, and their abilities to interact with Rab26 were determined in a GST fusion protein pulldown assay. The GST fusion proteins containing the ICL3, but not the ICL1, the ICL2 and the CT, were capable of interacting with Rab26 (Fig. 7*A*). The interaction of the ICL3 with wild-type Rab26 and its GTP-bound mutant Rab26Q123L was stronger than with the mutants Rab26T77N and Rab26N177I (Fig. 7*B*).

We then determined whether the interaction between Rab26 and the ICL3 is direct or indirect. Rab26 was expressed using an *in vitro* translation system, and its interaction with the ICL3 was determined by the GST fusion protein pulldown assay. The interaction of Rab26 with the GST-ICL3 was more potent in the present of GTPγS than in the presence of GDP (Fig. 7*C*), whereas the interaction between GST and Rab26 in the presence of GTPγS or GDP was undetectable. These data indicate that Rab26 directly interacts with the ICL3 of α_{2B}-AR, and the interaction largely depends on the activation of Rab26.

DISCUSSION

The molecular mechanisms underlying the anterograde transport of nascent GPCRs, especially from the Golgi to the cell surface, remain poorly elucidated. We have previously demonstrated the roles of Ras-like small GTPases and found that Rab1, Rab2, and Rab6 modulate the transport of GPCRs between the ER and the Golgi, whereas Rab8 and ARF1 are likely involved in receptor transport between the Golgi and the plasma membrane (18, 19, 27, 32–34). As a continuing effort to search for small GTPases in controlling export trafficking of GPCRs, in this study we have defined the role of Rab26 in the cell surface expression of GPCRs by focusing on α_2-ARs. Compared with many other secretory GTPases, Rab26 is relatively less well characterized. Rab26 was found to highly express in secretory cells and to regulate vesicle-mediated secretion (23, 24, 26). However, whether or not Rab26 is able to regulate the transport of plasma membrane proteins has not been studied. The data presented in this paper have clearly demonstrated that Rab26 modulates the cell surface transport of both α_{2A}-AR and α_{2B}-AR. By contrast, expression of several other secretory Rab GTPases, including Rab3A, Rab3B, Rab3C, Rab3D, Rab27A, Rab27B, and Rab37 in the same functional group (23–26, 35–40) did not influence the cell surface expression of α_2-ARs (data not shown). These data suggest that Rab26 is a unique secretory GTPase in this group that may function as a crucial regulator for the Golgi to cell surface movement of α_2-ARs. These data also provide the first evidence indicating that, in addition to its secretory function, Rab26 may play an important role in the transport of plasma membrane proteins, such as GPCRs.

In this study, the gain of Rab26 function was achieved by overexpression of Rab26, and the loss of Rab26 function achieved by transient expression of Rab26 mutants and siRNA-mediated depletion of endogenous Rab26. We have shown that expression of Rab26 mutants and siRNA-mediated knockdown of Rab26 significantly inhibited the cell surface expression of exogenously transfected α_2-ARs in HEK293 cells as well as endogenous α_2-ARs in MCF-7 cells. It is well known that the function of Rab GTPases in coordinating vesicular transport is mediated through their GTP/GDP exchange cycles. The inactive, GDP-bound conformation of Rab GTPases is maintained in the cytosol and undergoes GDP exchange for GTP. GTP-bound Rab will be hydrolyzed to the GDP-bound form for recycling back to donor membrane. Similar to the effect of GDP-bound mutant Rab26T77N and the guanine nucleotide binding-deficient Rab26N177I, expression of GTP-bound mutant Rab26Q123L inhibited the cell surface expression of α_2-ARs, suggesting that the recycling of Rab26 is an essential event in controlling the cell surface transport of α_2-ARs.

Expression of Rab26 mutants and Rab26 siRNA also attenuated α_2-AR-mediated signaling, specifically ERK1/2 activation. The reduction of α_2-AR-mediated ERK1/2 activation is presumably caused by the attenuation of receptor transport to the cell surface. However, we cannot exclude the possibility that inhibition of Rab26 function by expressing Rab26 mutants or Rab26 siRNA may alter α_2-AR coupling to other signaling molecules involved in receptor signaling systems, which may also contribute to the disruption of normal signal propagation of the receptors. By contrast, overexpression of Rab26 only moderately enhanced the cell surface numbers of α_2-ARs and receptor-mediated ERK1/2 activation, suggesting that the endogenous expression level of Rab26 may not be a rate-limiting factor for the cell surface transport of newly synthesized α_2-ARs. Nevertheless, these studies have strongly demonstrated for the first time that the small GTPase Rab26 plays a crucial role in the anterograde transport of α_2-ARs. However, whether or not Rab26 is involved in the cell surface transport of other GPCRs needs further investigation.

Rab26 likely modulates the cell surface transport of α_2-ARs from the Golgi. This became evident as α_{2B}-AR was extensively co-localized with the Golgi marker giantin in cells expressing the dominant-negative Rab26 mutants and Rab26 siRNA, indicating that attenuation of Rab26 function blocks the exit of newly synthesized α_{2B}-AR out of the Golgi apparatus. This notion is also supported by the localization of Rab26 in the Golgi. Interestingly, α_{2B}-AR was only partially accumulated in the Golgi in cells expressing the constitutively active GTP-bound mutant Rab26Q123L, suggesting that expression of Rab26Q123L may also arrest α_{2B}-AR in the post-Golgi compartments.

Another important finding presented in this manuscript is that, as determined by co-immunoprecipitation, BRET, and GST fusion protein pulldown assays, Rab26 directly and activation-dependently interacted with α_{2B}-AR, providing a possible molecular mechanism responsible for Rab26 regulation of post-Golgi traffic of α_2-ARs. There are a number of interesting points regarding the interaction between α_{2B}-AR and Rab26. First, the interaction of α_{2B}-AR with Rab26 depends on the activation of Rab26, which is in contrast to the interaction of β_2-AR and thromboxane A2 receptor with Rab11 (41, 42) and the interaction of α_{2B}-AR and β_2-AR with Rab8, which prefer the inactive GDP-bound Rab mutants (18). These data suggest α_{2B}-AR may be a downstream effector of Rab26 GTPase, because it has been well described that the downstream effectors strongly interact with the GTP-bound Rab GTPase mutants. Second, we have previously demonstrated that α_{2B}-AR uses its CT to associate with Rab8 (18), suggesting that α_{2B}-AR may utilize different intracellular domains to interact with distinct Rab GTPases (*i.e.*, the CT with Rab8 *versus* the ICL3 with Rab26). Because α_{2B}-AR preferentially interacts with the inactive form of Rab8 and the active form of Rab26, these interactions are likely to have different functions in modulating α_{2B}-AR export. Third, Rab26 represents the first Rab GTPase interacting with the ICL3 of GPCRs. Several other Rab GTPases have been shown to interact with the CTs of the receptors. For example, Rab4 and Rab11 interact with the CTs of angiotensin II type 1 receptor, β_2-AR, and thromboxane A2 receptor to regulate their recycling from endosomes back to the plasma membrane (41–43). Fourth, we have demonstrated that Rab26 generated by the *in vitro* translation system was able to interact with purified GST-ICL3 fusion proteins, suggesting that the interaction between α_{2B}-AR and Rab26 is direct. These data, together with other studies (18, 28, 41–43), suggest that the cargo GPCRs may physically bind to components of transport machinery, such as Rab GTPases, to control their transport to the cell surface.

The cell surface targeting of nascent GPCRs is one of the most important factors determining the functionality of the receptors and is directly linked to the pathogenesis of human diseases (44–47), including those essentially caused by naturally occurring mutations in the receptors resulting in the defective transport to the functional destination. Great progress has been achieved over the past several years in defining the role of small GTPases in the cell surface transport of GPCRs *en route* from the ER and the Golgi (17–19, 27, 32–34, 48–50). These studies have demonstrated that the proper receptor expression at the cell surface is tightly controlled by a number of small GTPases, each of which may regulate a specific step in the biosynthesis and processing of GPCRs. Because the dysfunction of Rab GTPases has also been implicated in the development of human diseases (51–54), to thoroughly explore the regulatory roles of small GTPases in the anterograde transport of nascent GPCRs, as well as possible underlying mechanisms, may reveal novel therapeutic targets for human diseases involving abnormal trafficking and signaling of GPCRs.

Acknowledgment—We thank Dr. Jianhui Guo for generating HEK293 cell lines stably expressing HA-α_{2B}-AR.

REFERENCES

1. Pierce, K. L., Premont, R. T., and Lefkowitz, R. J. (2002) Seven-transmembrane receptors. *Nat. Rev. Mol. Cell Biol.* **3,** 639–650
2. Kobilka, B. K. (2011) Structural insights into adrenergic receptor function and pharmacology. *Trends Pharmacol. Sci.* **32,** 213–218
3. Qin, K., Dong, C., Wu, G., and Lambert, N. A. (2011) Inactive-state preassembly of G_q-coupled receptors and G_q heterotrimers. *Nat. Chem. Biol.* **7,** 740–747
4. Dong, C., Filipeanu, C. M., Duvernay, M. T., and Wu, G. (2007) Regulation of G protein-coupled receptor export trafficking. *Biochim. Biophys. Acta* **1768,** 853–870
5. Wu, G., Krupnick, J. G., Benovic, J. L., and Lanier, S. M. (1997) Interaction of arrestins with intracellular domains of muscarinic and alpha2-adrenergic receptors. *J. Biol. Chem.* **272,** 17836–17842
6. Wu, G., Benovic, J. L., Hildebrandt, J. D., and Lanier, S. M. (1998) Receptor docking sites for G-protein $\beta\gamma$ subunits. Implications for signal regulation. *J. Biol. Chem.* **273,** 7197–7200
7. Tan, C. M., Brady, A. E., Nickols, H. H., Wang, Q., and Limbird, L. E. (2004) Membrane trafficking of G protein-coupled receptors. *Annu. Rev. Pharmacol. Toxicol.* **44,** 559–609
8. Xia, Z., Gray, J. A., Compton-Toth, B. A., and Roth, B. L. (2003) A direct interaction of PSD-95 with 5-HT2A serotonin receptors regulates receptor trafficking and signal transduction. *J. Biol. Chem.* **278,** 21901–21908
9. Hanyaloglu, A. C., and von Zastrow, M. (2008) Regulation of GPCRs by endocytic membrane trafficking and its potential implications. *Annu. Rev. Pharmacol. Toxicol.* **48,** 537–568
10. Moore, C. A., Milano, S. K., and Benovic, J. L. (2007) Regulation of receptor trafficking by GRKs and arrestins. *Annu. Rev. Physiol.* **69,** 451–482
11. Filipeanu, C. M., Zhou, F., Lam, M. L., Kerut, K. E., Claycomb, W. C., and

Wu, G. (2006) Enhancement of the recycling and activation of β-adrenergic receptor by Rab4 GTPase in cardiac myocytes. *J. Biol. Chem.* **281,** 11097–11103
12. Dong, C., and Wu, G. (2006) Regulation of anterograde transport of α_2-adrenergic receptors by the N termini at multiple intracellular compartments. *J. Biol. Chem.* **281,** 38543–38554
13. Daunt, D. A., Hurt, C., Hein, L., Kallio, J., Feng, F., and Kobilka, B. K. (1997) Subtype-specific intracellular trafficking of α2-adrenergic receptors. *Mol. Pharmacol.* **51,** 711–720
14. Venkatesan, S., Petrovic, A., Van Ryk, D. I., Locati, M., Weissman, D., and Murphy, P. M. (2002) Reduced cell surface expression of CCR5 in CCR5Δ32 heterozygotes is mediated by gene dosage, rather than by receptor sequestration. *J. Biol. Chem.* **277,** 2287–2301
15. Gimelbrant, A. A., Haley, S. L., and McClintock, T. S. (2001) Olfactory receptor trafficking involves conserved regulatory steps. *J. Biol. Chem.* **276,** 7285–7290
16. Zhu, L., Imanishi, Y., Filipek, S., Alekseev, A., Jastrzebska, B., Sun, W., Saperstein, D. A., and Palczewski, K. (2006) Autosomal recessive retinitis pigmentosa and E150K mutation in the opsin gene. *J. Biol. Chem.* **281,** 22289–22298
17. Wang, G., and Wu, G. (2012) Small GTPase regulation of GPCR anterograde trafficking. *Trends Pharmacol. Sci.* **33,** 28–34
18. Dong, C., Yang, L., Zhang, X., Gu, H., Lam, M. L., Claycomb, W. C., Xia, H., and Wu, G. (2010) Rab8 interacts with distinct motifs in α_{2B}- and β_2-adrenergic receptors and differentially modulates their transport. *J. Biol. Chem.* **285,** 20369–20380
19. Dong, C., Zhang, X., Zhou, F., Dou, H., Duvernay, M. T., Zhang, P., and Wu, G. (2010) ADP-ribosylation factors modulate the cell surface transport of G protein-coupled receptors. *J. Pharmacol. Exp. Ther.* **333,** 174–183
20. Deretic, D., Williams, A. H., Ransom, N., Morel, V., Hargrave, P. A., and Arendt, A. (2005) Rhodopsin C terminus, the site of mutations causing retinal disease, regulates trafficking by binding to ADP-ribosylation factor 4 (ARF4). *Proc. Natl. Acad. Sci. U.S.A.* **102,** 3301–3306
21. Mazelova, J., Astuto-Gribble, L., Inoue, H., Tam, B. M., Schonteich, E., Prekeris, R., Moritz, O. L., Randazzo, P. A., and Deretic, D. (2009) Ciliary targeting motif VxPx directs assembly of a trafficking module through Arf4. *EMBO J.* **28,** 183–192
22. Luo, W., Wang, Y., and Reiser, G. (2007) p24A, a type I transmembrane protein, controls ARF1-dependent resensitization of protease-activated receptor-2 by influence on receptor trafficking. *J. Biol. Chem.* **282,** 30246–30255
23. Yoshie, S., Imai, A., Nashida, T., and Shimomura, H. (2000) Expression, characterization, and localization of Rab26, a low molecular weight GTP-binding protein, in the rat parotid gland. *Histochem. Cell Biol.* **113,** 259–263
24. Nashida, T., Imai, A., and Shimomura, H. (2006) Relation of Rab26 to the amylase release from rat parotid acinar cells. *Arch. Oral Biol.* **51,** 89–95
25. Fukuda, M. (2003) Distinct Rab binding specificity of Rim1, Rim2, rabphilin, and Noc2. Identification of a critical determinant of Rab3A/Rab27A recognition by Rim2. *J. Biol. Chem.* **278,** 15373–15380
26. Tian, X., Jin, R. U., Bredemeyer, A. J., Oates, E. J., Blazewska, K. M., McKenna, C. E., and Mills, J. C. (2010) RAB26 and RAB3D are direct transcriptional targets of MIST1 that regulate exocrine granule maturation. *Mol. Cell. Biol.* **30,** 1269–1284
27. Wu, G., Zhao, G., and He, Y. (2003) Distinct pathways for the trafficking of angiotensin II and adrenergic receptors from the endoplasmic reticulum to the cell surface. Rab1-independent transport of a G protein-coupled receptor. *J. Biol. Chem.* **278,** 47062–47069
28. Dong, C., Nichols, C. D., Guo, J., Huang, W., Lambert, N. A., and Wu, G. (2012) A triple arg motif mediates α_{2B}-adrenergic receptor interaction with Sec24C/D and export. *Traffic* **13,** 857–868
29. Duvernay, M. T., Dong, C., Zhang, X., Robitaille, M., Hébert, T. E., and Wu, G. (2009) A single conserved leucine residue on the first intracellular loop regulates ER export of G protein-coupled receptors. *Traffic* **10,** 552–566
30. Duvernay, M. T., Dong, C., Zhang, X., Zhou, F., Nichols, C. D., and Wu, G. (2009) Anterograde trafficking of G protein-coupled receptors. Function of the C-terminal F_X6LL motif in export from the endoplasmic reticulum. *Mol. Pharmacol.* **75,** 751–761
31. Lan, T. H., Liu, Q., Li, C., Wu, G., and Lambert, N. A. (2012) Sensitive and high resolution localization and tracking of membrane proteins in live cells with BRET. *Traffic* **13,** 1450–1456
32. Filipeanu, C. M., Zhou, F., Claycomb, W. C., and Wu, G. (2004) Regulation of the cell surface expression and function of angiotensin II type 1 receptor by Rab1-mediated endoplasmic reticulum-to-Golgi transport in cardiac myocytes. *J. Biol. Chem.* **279,** 41077–41084
33. Filipeanu, C. M., Zhou, F., Fugetta, E. K., and Wu, G. (2006) Differential regulation of the cell-surface targeting and function of β- and α_1-adrenergic receptors by Rab1 GTPase in cardiac myocytes. *Mol. Pharmacol.* **69,** 1571–1578
34. Dong, C., and Wu, G. (2007) Regulation of anterograde transport of adrenergic and angiotensin II receptors by Rab2 and Rab6 GTPases. *Cell Signal.* **19,** 2388–2399
35. Wagner, A. C., Strowski, M. Z., Göke, B., and Williams, J. A. (1995) Molecular cloning of a new member of the Rab protein family, Rab 26, from rat pancreas. *Biochem. Biophys. Res. Commun.* **207,** 950–956
36. Bustos, M. A., Lucchesi, O., Ruete, M. C., Mayorga, L. S., and Tomes, C. N. (2012) Rab27 and Rab3 sequentially regulate human sperm dense-core granule exocytosis. *Proc. Natl. Acad. Sci. U.S.A.* **109,** E2057–2066
37. Tsuboi, T., and Fukuda, M. (2006) Rab3A and Rab27A cooperatively regulate the docking step of dense-core vesicle exocytosis in PC12 cells. *J. Cell Sci.* **119,** 2196–2203
38. Fukuda, M. (2008) Regulation of secretory vesicle traffic by Rab small GTPases. *Cell. Mol. Life Sci.* **65,** 2801–2813
39. Masuda, E. S., Luo, Y., Young, C., Shen, M., Rossi, A. B., Huang, B. C., Yu, S., Bennett, M. K., Payan, D. G., and Scheller, R. H. (2000) Rab37 is a novel mast cell specific GTPase localized to secretory granules. *FEBS Lett.* **470,** 61–64
40. Pereira-Leal, J. B., and Seabra, M. C. (2001) Evolution of the Rab family of small GTP-binding proteins. *J. Mol. Biol.* **313,** 889–901
41. Parent, A., Hamelin, E., Germain, P., and Parent, J. L. (2009) Rab11 regulates the recycling of the β_2-adrenergic receptor through a direct interaction. *Biochem. J.* **418,** 163–172
42. Hamelin, E., Thériault, C., Laroche, G., and Parent, J. L. (2005) The intracellular trafficking of the G protein-coupled receptor TPβ depends on a direct interaction with Rab11. *J. Biol. Chem.* **280,** 36195–36205
43. Seachrist, J. L., Laporte, S. A., Dale, L. B., Babwah, A. V., Caron, M. G., Anborgh, P. H., and Ferguson, S. S. (2002) Rab5 association with the angiotensin II type 1A receptor promotes Rab5 GTP binding and vesicular fusion. *J. Biol. Chem.* **277,** 679–685
44. Morello, J. P., and Bichet, D. G. (2001) Nephrogenic diabetes insipidus. *Annu Rev Physiol* **63,** 607–630
45. Stojanovic, A., and Hwa, J. (2002) Rhodopsin and retinitis pigmentosa. Shedding light on structure and function. *Receptors Channels* **8,** 33–50
46. Themmen, A. P., and Brunner, H. G. (1996) Luteinizing hormone receptor mutations and sex differentiation. *Eur. J. Endocrinol.* **134,** 533–540
47. Sánchez-Laorden, B. L., Herraiz, C., Valencia, J. C., Hearing, V. J., Jiménez-Cervantes, C., and García-Borrón, J. C. (2009) Aberrant trafficking of human melanocortin 1 receptor variants associated with red hair and skin cancer. Steady-state retention of mutant forms in the proximal golgi. *J. Cell. Physiol.* **220,** 640–654
48. Madziva, M. T., and Birnbaumer, M. (2006) A role for ADP-ribosylation factor 6 in the processing of G-protein-coupled receptors. *J. Biol. Chem.* **281,** 12178–12186
49. Zhuang, X., Adipietro, K. A., Datta, S., Northup, J. K., and Ray, K. (2010) Rab1 small GTP-binding protein regulates cell surface trafficking of the human calcium-sensing receptor. *Endocrinology* **151,** 5114–5123
50. Conn, P. M., Ulloa-Aguirre, A., Ito, J., and Janovick, J. A. (2007) G protein-coupled receptor trafficking in health and disease. Lessons learned to prepare for therapeutic mutant rescue *in vivo*. *Pharmacol. Rev.* **59,** 225–250
51. Charron, A. J., Bacallao, R. L., and Wandinger-Ness, A. (2000) ADPKD. A human disease altering Golgi function and basolateral exocytosis in renal epithelia. *Traffic* **1,** 675–686
52. Wu, G., Yussman, M. G., Barrett, T. J., Hahn, H. S., Osinska, H., Hill-

iard, G. M., Wang, X., Toyokawa, T., Yatani, A., Lynch, R. A., Robbins, J., and Dorn, G. W., 2nd (2001) Increased myocardial Rab GTPase expression. A consequence and cause of cardiomyopathy. *Circ. Res.* **89,** 1130–1137

53. Ménasché, G., Pastural, E., Feldmann, J., Certain, S., Ersoy, F., Dupuis, S., Wulffraat, N., Bianchi, D., Fischer, A., Le Deist, F., and de Saint Basile, G. (2000) Mutations in RAB27A cause Griscelli syndrome associated with haemophagocytic syndrome. *Nat. Genet.* **25,** 173–176
54. Cheng, K. W., Lahad, J. P., Kuo, W. L., Lapuk, A., Yamada, K., Auersperg, N., Liu, J., Smith-McCune, K., Lu, K. H., Fishman, D., Gray, J. W., and Mills, G. B. (2004) The RAB25 small GTPase determines aggressiveness of ovarian and breast cancers. *Nat. Med.* **10,** 1251–1256